PHYSICAL REVIEW D **77,** 051901(R) (2008)

Polyakov loop extended Nambu–Jona-Lasinio model with imaginary chemical potential

Yuji Sakai,[1,*] Kouji Kashiwa,[1,†] Hiroaki Kouno,[2,‡] and Masanobu Yahiro[1,§]

[1]*Department of Physics, Graduate School of Sciences, Kyushu University, Fukuoka 812-8581, Japan*

[2]*Department of Physics, Saga University, Saga 840-8502, Japan*

(Received 29 December 2007; published 7 March 2008)

The Polyakov loop extended Nambu–Jona-Lasinio (PNJL) model with imaginary chemical potential is studied. The model possesses the extended $\mathbb{Z}_3$ symmetry that QCD does. Quantities invariant under the extended $\mathbb{Z}_3$ symmetry, such as the partition function, the chiral condensate, and the modified Polyakov loop, have Roberge-Weiss periodicity. The phase diagram of confinement/deconfinement transition derived with the PNJL model is consistent with the Roberge-Weiss prediction on it and the results of lattice QCD. The phase diagram of chiral transition is also presented by the PNJL model.

DOI: 10.1103/PhysRevD.77.051901 PACS numbers: 11.30.Rd, 12.40.−y

With the aid of the progress in computer power, lattice QCD simulations have become feasible for thermal systems at zero quark chemical potential (μ) [1]. As for $\mu > 0$, however, lattice QCD has the well-known sign problem, and then the results are still far from perfection; for example, see Ref. [2] and references therein.

Several approaches have been proposed to solve the sign problem. One of them is the use of imaginary chemical potential, since the fermionic determinant that appears in the Euclidean partition function is real in the case; for example, see Refs. [3–5] and references therein. If the physical quantity such as chiral condensate is known in the imaginary μ region, one can extrapolate it to the real μ region, until a discontinuity appears. Furthermore, in principle, one can evaluate with the Fourier transformation the canonical partition function with fixed quark number from the grand canonical partition function with imaginary chemical potential [6].

Roberge and Weiss (RW) [6] found that the partition function of SU(N) gauge theory with imaginary chemical potential $\mu = i\theta/\beta$,

$$Z(\theta) = \int D\psi D\bar{\psi} DA_\mu \exp\Big[- \int d^4x \Big\{ \bar{\psi}(\gamma D - m_0)\psi - \frac{1}{4} F_{\mu\nu}^2 - i\frac{\theta}{\beta}\bar{\psi}\gamma_4\psi \Big\} \Big], \tag{1}$$

is a periodic function of θ with a period $2\pi/N$, that is, $Z(\theta + 2\pi k/N) = Z(\theta)$ for any integer k, by showing that $Z(\theta + 2\pi k/N)$ is reduced to $Z(\theta)$ with the $\mathbb{Z}_N$ transformation,

$$\psi \to U\psi, \qquad A_\nu \to UA_\nu U^{-1} - \frac{i}{g}(\partial_\nu U)U^{-1}, \tag{2}$$

where $U(x, \tau)$ are elements of SU(N) with the boundary condition $U(x, \beta) = \exp(-2i\pi k/N)U(x, 0)$. Here ψ is the fermion field with mass m_0, $F_{\mu\nu}$ is the strength tensor of the gauge field A_μ, and β is the inverse of temperature T. The RW periodicity means that $Z(\theta)$ is invariant under the extended $\mathbb{Z}_N$ transformation,

$$\theta \to \theta + \tfrac{2\pi k}{N}, \qquad \psi \to U\psi, \qquad A_\nu \to UA_\nu U^{-1} - \tfrac{i}{g}(\partial_\nu U)U^{-1}. \tag{3}$$

Quantities invariant under the extended $\mathbb{Z}_N$ transformation, such as the thermodynamic potential $\Omega(\theta)$ and the chiral condensate, keep the RW periodicity. Meanwhile, the Polyakov loop Φ is not invariant under the transformation (3), since it is transformed as $\Phi \to \Phi e^{-i2\pi k/N}$. In general, noninvariant quantities such as Φ do not have the periodicity. Roberge and Weiss also showed with perturbation that in the high T region $d\Omega(\theta)/d\theta$ and Φ are discontinuous as a function of θ at values of $(2k + 1)\pi/N$, and also found with the strongly coupled lattice theory that the discontinuities disappear in the low T region. This is called the Roberge-Weiss phase transition of first order, and is observed in lattice simulations [3–5].

Figure 1 shows a predicted phase diagram in the θ-T plane. The solid lines represent the RW discontinuities of the Polyakov loop, and the dot-dashed lines show the chiral phase transition predicted by the lattice simulations, although results of the simulations are not conclusive yet since it is hard to take the chiral limit in the simulations. The RW transition is the first-order one appearing in Φ, but not an ordinary first-order confinement/deconfinement transition. Although both are defined by discontinuities of Φ, the latter is a jump of $|\Phi|$ from almost zero to a finite value, but the former is a discontinuity of Φ in its phase, as shown later.

As an approach complementary to first-principle lattice simulations, one can consider several effective models. One of them is the Nambu–Jona-Lasinio (NJL) model [7]. Although the NJL model is a useful method for understanding chiral symmetry breaking, this model does not possess a confinement mechanism. As a reliable model that can treat both the chiral and the deconfinement phase transitions, we can consider the Polyakov loop extended

*sakai2scp@mbox.nc.kyushu-u.ac.jp
†kashiwa2scp@mbox.nc.kyushu-u.ac.jp
‡kounoh@cc.saga-u.ac.jp
§yahiro2scp@mbox.nc.kyushu-u.ac.jp

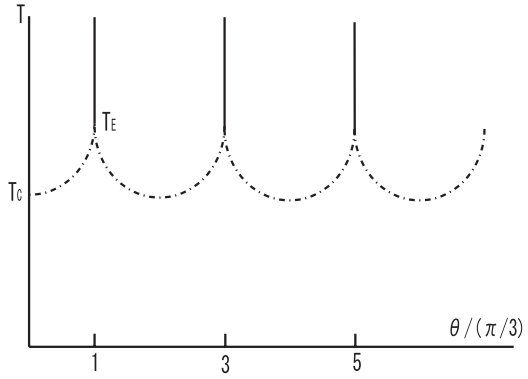

FIG. 1. The RW prediction on the QCD phase diagram in the θ-T plane.

NJL (PNJL) model [8–20]. In the PNJL model the deconfinement phase transition is described by the Polyakov loop. It is known that effects of the Polyakov loop make the critical endpoint [21–23] move to higher T and lower μ than the NJL model predicts [16,20].

The PNJL model has the extended $\mathbb{Z}_3$ symmetry needed to reproduce the RW periodicity, as shown later. In this paper, we study the phase diagram in the θ-T plane by using the PNJL model. Both the chiral and the deconfinement phase transitions are analyzed in the chiral ($m_0 = 0$) limit, where the lattice simulation is not available.

The model we consider is the following two-flavor PNJL Lagrangian,

$$\mathcal{L} = \bar{q}(i\gamma_\nu D^\nu - m_0)q + G_{\rm s}[(\bar{q}q)^2 + (\bar{q}i\gamma_5\vec{\tau}q)^2] - \mathcal{U}(\Phi[A], \Phi[A]^*, T), \tag{4}$$

where q denotes the two-flavor quark field, m_0 does the current quark mass, and $D^\nu = \partial^\nu - iA^\nu - i\delta^\nu_0\mu$ for the chemical potential $\mu = i\theta/\beta$. The field A^ν is defined as $A^\nu = \delta_{\nu 0} g A^\nu_a \frac{\lambda^a}{2}$ with the gauge field A^ν_a, the Gell-Mann matrix λ_a, and the gauge coupling g. In the NJL sector, $\vec{\tau}$ stands for the isospin matrix, and $G_{\rm s}$ denotes the coupling constant of the scalar-type four-quark interaction. The Polyakov potential $\mathcal{U}$, defined later in (11), is a function of the Polyakov loop Φ and its complex conjugate Φ^*,

$$\Phi = \frac{1}{N_{\rm c}}{\rm Tr}L, \qquad \Phi^* = \frac{1}{N_{\rm c}}{\rm Tr}L^\dagger, \tag{5}$$

with

$$L(\mathbf{x}) = \mathcal{P}\exp\left[i\int_0^\beta d\tau A_4(\mathbf{x},\tau)\right], \tag{6}$$

where $\mathcal{P}$ is the path ordering, $A_4 = iA_0$, and $N_c = 3$. In the chiral limit ($m_0 = 0$), the Lagrangian density has the exact $SU(2)_{\rm L} \times SU(2)_{\rm R} \times U(1)_{\rm v} \times SU(3)_{\rm c}$ symmetry.

The temporal component A_4 is diagonal in the flavor space, because the color and the flavor space are completely separated out in the present case. In the Polyakov gauge, L can be written in a diagonal form in the color space [10]:

$$L = e^{i\beta(\phi_3\lambda_3 + \phi_8\lambda_8)} = {\rm diag}(e^{i\beta\phi_a}, e^{i\beta\phi_b}, e^{i\beta\phi_c}), \tag{7}$$

where $\phi_a = \phi_3 + \phi_8/\sqrt{3}$, $\phi_b = -\phi_3 + \phi_8/\sqrt{3}$, and $\phi_c = -(\phi_a + \phi_b) = -2\phi_8/\sqrt{3}$. The Polyakov loop Φ is an exact order parameter of the spontaneous $\mathbb{Z}_3$ symmetry breaking in the pure gauge theory. Although the $\mathbb{Z}_3$ symmetry is not exact in the system with dynamical quarks, it still seems to be a good indicator of the deconfinement phase transition. Therefore, we use Φ to define the deconfinement phase transition.

Under the mean field approximation (MFA), the Lagrangian density becomes

$$\mathcal{L}_{\rm MFA} = \bar{q}(i\gamma_\mu D^\mu - (m_0 + \Sigma_{\rm s}))q - U(\sigma) - \mathcal{U}(\Phi, \Phi^*, T), \tag{8}$$

where

$$\sigma = \langle\bar{q}q\rangle, \qquad \Sigma_{\rm s} = -2G_{\rm s}\sigma, \qquad U = G_{\rm s}\sigma^2. \tag{9}$$

Using the usual techniques, one can obtain the thermodynamic potential

$$\Omega = -2N_f V\int\frac{d^3{\rm p}}{(2\pi)^3}\Big[3E({\rm p}) + \frac{1}{\beta}\ln[1 + 3(\Phi + \Phi^* e^{-\beta E^-(\mathbf{p})})e^{-\beta E^-(\mathbf{p})} + e^{-3\beta E^-(\mathbf{p})}] + \frac{1}{\beta}\ln[1 + 3(\Phi^* + \Phi e^{-\beta E^+(\mathbf{p})})e^{-\beta E^+(\mathbf{p})} + e^{-3\beta E^+(\mathbf{p})}]\Big] + (U + \mathcal{U})V, \tag{10}$$

where $E({\rm p}) = \sqrt{\mathbf{p}^2 + M^2}$, $E^\pm({\rm p}) = E({\rm p}) \pm i\theta/\beta$, and $M = m_0 + \Sigma_{\rm s}$. We use $\mathcal{U}$ of Ref. [13] which is fitted to the result of lattice simulation in the pure gauge theory at finite T [24,25]:

$$\frac{\mathcal{U}}{T^4} = -\frac{b_2(T)}{2}\Phi^*\Phi - \frac{b_3}{6}(\Phi^{*3} + \Phi^3) + \frac{b_4}{4}(\Phi^*\Phi)^2, \tag{11}$$

$$b_2(T) = a_0 + a_1\left(\frac{T_0}{T}\right) + a_2\left(\frac{T_0}{T}\right)^2 + a_3\left(\frac{T_0}{T}\right)^3, \tag{12}$$

where parameters are summarized in Table I. The Polyakov potential yields a deconfinement phase transition at $T = T_0$ in the pure gauge theory. Hence, T_0 is taken to be 270 MeV, predicted by the pure gauge lattice QCD calculation.

The variables of Φ, Φ^*, and σ satisfy the stationary conditions,

$$\partial\Omega/\partial\Phi = 0, \qquad \partial\Omega/\partial\Phi^* = 0, \qquad \partial\Omega/\partial\sigma = 0. \tag{13}$$

The thermodynamic potential $\Omega(\theta)$ at each θ is obtained by

TABLE I. Summary of the parameter set in the Polyakov sector used in Ref. [13]. All parameters are dimensionless.

a_0	a_1	a_2	a_3	b_3	b_4
6.75	−1.95	2.625	−7.44	0.75	7.5

inserting the solutions, $\Phi(\theta)$, $\Phi(\theta)^*$, and $\sigma(\theta)$, of (13) at each θ into (10).

The thermodynamic potential Ω is not invariant under the $\mathbb{Z}_3$ transformation, $\Phi(\theta) \to \Phi(\theta)e^{-i2\pi k/3}$ and $\Phi(\theta)^* \to \Phi(\theta)^* e^{i(2\pi k/3)}$, although $\mathcal{U}$ of (11) is invariant. Instead of the $\mathbb{Z}_3$ symmetry, however, Ω is invariant under the extended $\mathbb{Z}_3$ transformation,

$$e^{\pm i\theta} \to e^{\pm i\theta} e^{\pm i(2\pi k/3)}, \qquad \Phi(\theta) \to \Phi(\theta) e^{-i(2\pi k/3)}, \qquad \Phi(\theta)^* \to \Phi(\theta)^* e^{i(2\pi k/3)}. \tag{14}$$

It is convenient to introduce new variables $\Psi \equiv e^{i\theta}\Phi$ and $\Psi^* \equiv e^{-i\theta}\Phi^*$ invariant under the transformation (14).

The extended $\mathbb{Z}_3$ transformation is then rewritten into

$$e^{\pm i\theta} \to e^{\pm i\theta} e^{\pm i(2\pi k/3)}, \qquad \Psi(\theta) \to \Psi(\theta), \qquad \Psi(\theta)^* \to \Psi(\theta)^*, \tag{15}$$

and Ω is also rewritten into

$$\begin{aligned}\Omega = & -2N_f V \int \frac{d^3\mathrm{p}}{(2\pi)^3}\Big[3E(\mathrm{p}) + \frac{1}{\beta}\ln[1 + 3\Psi e^{-\beta E(\mathrm{p})} \\ & + 3\Psi^* e^{-2\beta E(\mathrm{p})} e^{\beta\mu_\mathrm{B}} + e^{-3\beta E(\mathrm{p})} e^{\beta\mu_\mathrm{B}}] \\ & + \frac{1}{\beta}\ln[1 + 3\Psi^* e^{-\beta E(\mathrm{p})} + 3\Psi e^{-2\beta E(\mathrm{p})} e^{-\beta\mu_\mathrm{B}} \\ & + e^{-3\beta E(\mathrm{p})} e^{-\beta\mu_\mathrm{B}}]\Big] + UV + \Big[-\frac{b_2(T)T^4}{2}\Psi^*\Psi \\ & - \frac{\beta_3(T)T^4}{6}(\Psi^{*3} e^{\beta\mu_\mathrm{B}} + \Psi^3 e^{-\beta\mu_\mathrm{B}}) \\ & + \frac{b_4 T^4}{4}(\Psi^*\Psi)^2\Big]V,\end{aligned} \tag{16}$$

where $\mu_\mathrm{B} = 3\mu = i3\theta/\beta$ is the baryonic chemical potential and the factor $e^{\pm\beta\mu_\mathrm{B}}$ is invariant under the transformation (15). Obviously, Ω is invariant under the transformation (15).

Under the transformation $\theta \to \theta + 2\pi k/3$, (16) keeps the same form, if $\Psi(\theta)$ and $\Psi(\theta)^*$ are replaced by $\Psi(\theta + 2\pi k/3)$ and $\Psi(\theta + 2\pi k/3)^*$, respectively. This means that the stationary conditions for $\Psi(\theta)$ and $\Psi(\theta)^*$ agree with those for $\Psi(\theta + 2\pi k/3)$ and $\Psi(\theta + 2\pi k/3)^*$, respectively, and then

$$\Psi\left(\theta + \tfrac{2\pi k}{3}\right) = \Psi(\theta) \quad \text{and} \quad \Psi\left(\theta + \tfrac{2\pi k}{3}\right)^* = \Psi(\theta)^*. \tag{17}$$

The potential Ω depends on θ through $\Psi(\theta)$, $\Psi(\theta)^*$, $\sigma(\theta)$, and $e^{i\theta}$. We then denote $\Omega(\theta)$ by $\Omega(\theta) = \Omega(\Psi(\theta), \Psi(\theta)^*, e^{i\theta})$, where $\sigma(\theta)$ is suppressed since it is irrelevant to the proofs shown below. The RW periodicity of Ω is then shown as

$$\begin{aligned}\Omega\left(\theta + \frac{2\pi k}{3}\right) &= \Omega(\Psi(\theta), \Psi(\theta)^*, e^{i(2\pi k/3) + i\theta}) \\ &= \Omega(\Psi(\theta), \Psi(\theta)^*, e^{i\theta}) = \Omega(\theta),\end{aligned} \tag{18}$$

by using (17) in the first equality and the extended $\mathbb{Z}_3$ symmetry of Ω in the second equality.

Equation (16) keeps the same form under the transformation $\theta \to -\theta$, if $\Psi(\theta)$ and $\Psi(\theta)^*$ are replaced by $\Psi(-\theta)^*$ and $\Psi(-\theta)$, respectively. This indicates that

$$\Psi(-\theta) = \Psi(\theta)^* \quad \text{and} \quad \Psi(-\theta)^* = \Psi(\theta). \tag{19}$$

Furthermore, Ω is a real function, as shown in (16). Using these properties, one can show that

$$\begin{aligned}\Omega(\theta) &= (\Omega(\theta))^* = \Omega(\Psi(\theta)^*, \Psi(\theta), e^{-i\theta}) \\ &= \Omega(\Psi(-\theta), \Psi(-\theta)^*, e^{-i\theta}) = \Omega(-\theta).\end{aligned} \tag{20}$$

Thus, Ω is a periodic even function of θ with a period $2\pi/3$. The chiral condensate $\sigma(\theta)$ is also a periodic even function of θ, $\sigma(\theta) = \sigma(\theta + 2\pi k/3) = \sigma(-\theta)$, because it is given by $\sigma(\theta) = d\Omega(\theta)/dm_0$.

The modified Polyakov loop Ψ has a periodicity of (17). The real (imaginary) part of Ψ is even (odd) under the interchange $\theta \leftrightarrow -\theta$, because of (19): $\mathrm{Re}[\Psi(\theta)] = (\Psi(\theta) + \Psi(\theta)^*)/2 = \mathrm{Re}[\Psi(-\theta)]$ and $\mathrm{Im}[\Psi(\theta)] = (\Psi(\theta) - \Psi(\theta)^*)/(2i) = -\mathrm{Im}[\Psi(-\theta)]$. Thus, the real (imaginary) part of Ψ is a periodic even (odd) function of θ.

Since $\Omega(\theta)$, $\Psi(\theta)$, and $\sigma(\theta)$ are periodic functions of θ with a period $2\pi/3$, here we think a period $0 \le \theta \le 2\pi/3$. In the region, periodic even functions such as $\Omega(\theta)$, $\sigma(\theta)$, and $\mathrm{Re}[\Psi(\theta)]$ are symmetric with respect to a line $\theta = \pi/3$. This indicates that such an even function has a cusp at $\theta = \pi/3$, if the gradient $\lim_{\theta\to\pi/3\pm 0} d\Omega/d\theta$ is neither zero nor infinity. Such a cusp comes out in the high T region, as shown later with numerical calculations. This means that the chiral phase transition at $\theta = \pi/3$ is the second order.

Meanwhile, $\mathrm{Im}[\Psi(\theta)]$ is a periodic odd function, so that $\mathrm{Im}[\Psi(\pi/3 - \epsilon)] = -\mathrm{Im}[\Psi(-\pi/3 + \epsilon)] = -\mathrm{Im}[\Psi(\pi/3 + \epsilon)]$ for positive infinitesimal ϵ. This indicates that $\mathrm{Im}[\Psi(\theta)]$ is discontinuous at $\theta = \pi/3$, if it is not zero there. This is the RW phase transition, which is seen in the high T region, as shown later. The phase of Ψ, $\arctan[\mathrm{Im}(\Psi)/\mathrm{Re}(\Psi)]$, has the same property as the imaginary part, since the phase is obviously a periodic odd function. Thus, the RW transition at $\theta = \pi/3$ is the first-order one appearing in the imaginary part of Ψ and the phase of Ψ.

Since the NJL model is nonrenormalizable, one then needs to introduce a cutoff in the momentum integration.

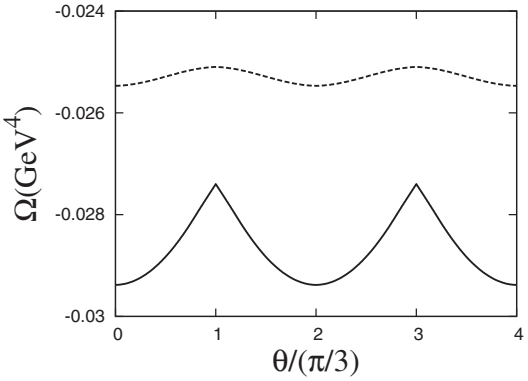

FIG. 2. Thermodynamic potential Ω as a function of θ. The solid line represents a result of the case of $T = 300$ MeV, and the dashed one corresponds to that of $T = 250$ MeV.

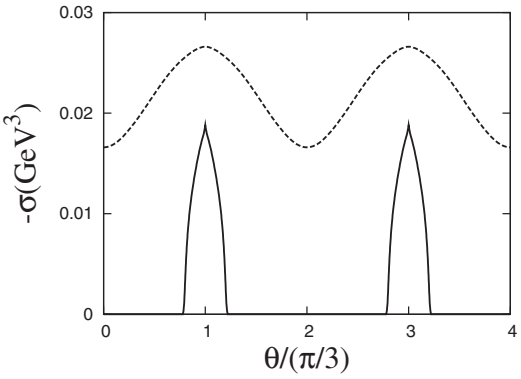

FIG. 4. Chiral condensate σ as a function of θ. The definitions of the lines are the same as in Fig. 2.

Here we take the three-dimensional momentum cutoff Λ. Hence, the present model has three parameters, m_0, Λ, G_s, in the NJL sector. Following Ref. [23], we take $\Lambda = 0.6315$ GeV and $G_s = 5.498$ GeV^{-2}, although we consider the chiral limit ($m_0 = 0$).

Figure 2 shows Ω as a function of θ in two cases of $T = 250$ MeV and 300 MeV. The potential Ω is smooth everywhere in the low T case, but not at $\theta = (2k + 1)\pi/3$ in the high T case. This result is consistent with the RW prediction [6] and lattice simulation [4] on the θ and the T dependence of the QCD thermodynamic potential.

Figure 3 shows the real and imaginary parts of the modified Polyakov loop $\Psi(\theta)$. In the case of $T = 300$ MeV, the imaginary part of $\Psi(\theta)$ is discontinuous at $\theta = (2k + 1)\pi/3$, while the real part of $\Psi(\theta)$ is continuous but not smooth there. Thus, the phase transition of first order appears at $\theta = (2k + 1)\pi/3$ in the high T region. This is precisely the RW phase transition. In the case of $T = 250$ MeV, meanwhile, both the real and the imaginary parts are smooth everywhere. All the results on the θ and the T dependence of Ψ are consistent with the RW prediction on it and the results of lattice simulations [3–5].

Figure 4 shows the chiral condensate σ as a function of θ. In the case of $T = 300$ MeV, σ has a cusp at each of $\theta = (2k + 1)\pi/3$. Thus, the phase transition of second order comes out at $\theta = (2k + 1)\pi/3$. Meanwhile, in the case of $T = 250$ MeV, there is no cusp at $\theta = (2k + 1)\pi/3$, indicating no phase transition there.

Figure 5 represents the phase diagram in the θ-T plane. The phase diagram is symmetric with respect to each of lines $\theta = k\pi/3$ for any integer k. The dashed curve between D and E represents the deconfinement phase transition of crossover, and the dot-dashed curve between C and F shows the second-order chiral phase transition. Thus, for $\theta \neq k\pi/3$ the chiral phase transition occurs at higher T than the deconfinement phase transition does. The solid vertical line starting from point E represents the first-order RW transition of Ψ. Both the RW and the chiral phase transitions occur on the line between E and F, although the RW transition is first order and the chiral one is second order there. Point F turns out to be a bifurcation of the chiral phase transition line, and point E is an endpoint of the RW phase transition.

Temperatures of C, D, E, F are about 261 MeV, 240 MeV, 269 MeV, 328 MeV, respectively. Thus, at $\theta = 0$ the critical temperature of the chiral phase transition is higher by about 20 MeV than that of the deconfinement transition, and the difference is getting larger gradually as θ increases to $\pi/3$. Meanwhile, the lattice simulation suggests that the two critical temperatures are almost identical, not only for zero θ but also for finite θ [4]. The

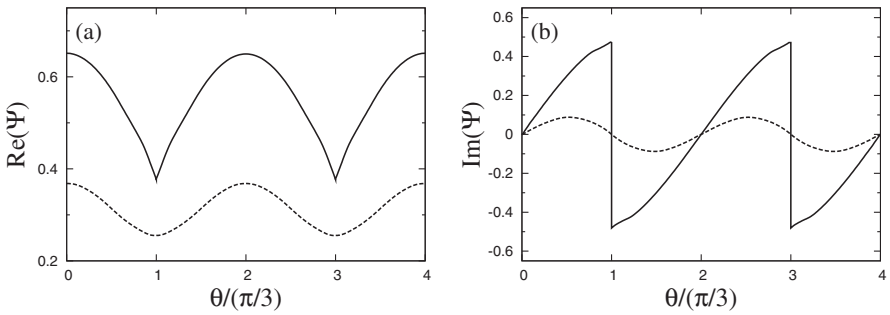

FIG. 3. The modified Polyakov loop $\Psi(\theta)$ as a function of θ: (a) for the real part and (b) for the imaginary part. The definitions of the lines are the same as in Fig. 2.

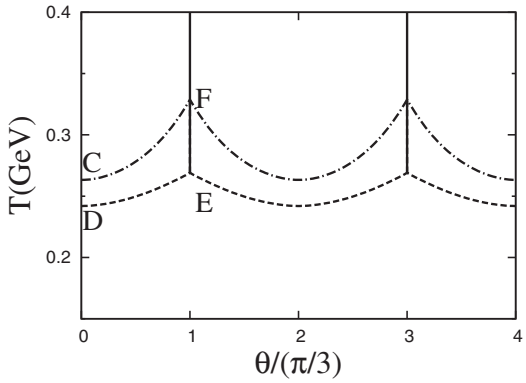

FIG. 5. The phase diagram in the θ-T plane.

difference between the two critical temperatures, seen in Fig. 5, is reduced by a factor 3 by adding the scalar-type eight-quark interaction to the PNJL Lagrangian [20].

There are some ambiguities in the PNJL model, for example, the form of the Polyakov potential $\mathcal{U}$ and the value of T_0. For $\mathcal{U}$, the logarithmic form of [15,16] may be more appropriate when $|\Phi|$ is large. For T_0, it may be more reasonable to take a lower value, say $\sim$180 MeV, determined from lattice simulations with dynamical quarks [13,20,26], instead of the present one, 270 MeV, from the pure gauge lattice simulation. The lower value of T_0 shifts both the chiral and deconfinement transition lines toward lower T. Further discussions on these will be made in the forthcoming paper.

The success of the PNJL model comes from the fact that the PNJL model has the extended $\mathbb{Z}_3$ symmetry, or more precisely, that the thermodynamic potential (16) is a function only of variables, Ψ, Ψ^*, $e^{\pm\beta\mu_B}$, and σ, invariant under the extended $\mathbb{Z}_3$ symmetry. A reliable effective theory of QCD proposed in the future is expected to have the same property in its thermodynamic potential. This may be a good guiding principle to elaborate an effective theory of QCD.

The authors thank M. Matsuzaki, T. Murase, M. Imachi, H. Yoneyama, and M. Tachibana for useful discussions. This work has been supported in part by the Grants-in-Aid for Scientific Research (No. 18540280) of Education, Science, Sports, and Culture of Japan.

[1] J. Kogut, M. Stone, H. W. Wyld, W. R. Gibbs, J. Shigemitsu, S. H. Shenker, and D. K. Sinclair, Phys. Rev. Lett. **50**, 393 (1983).
[2] J. B. Kogut and D. K. Sinclair, arXiv:hep-lat/0712.2625.
[3] P. de Forcrand and O. Philipsen, Nucl. Phys. **B642**, 290 (2002); **B673**, 170 (2003).
[4] M. D'Elia and M. P. Lombardo, Phys. Rev. D **67**, 014505 (2003); **70**, 074509 (2004); M. P. Lombardo, Proc. Sci., CPOD2006 (2006) 003 [arXiv:hep-lat/0612017].
[5] H. S. Chen and X. Q. Luo, Phys. Rev. D **72**, 034504 (2005).
[6] A. Roberge and N. Weiss, Nucl. Phys. **B275**, 734 (1986).
[7] Y. Nambu and G. Jona-Lasinio, Phys. Rev. **122**, 345 (1961); **124**, 246 (1961).
[8] P. N. Meisinger and M. C. Ogilvie, Phys. Lett. B **379**, 163 (1996).
[9] A. Dumitru and R. D. Pisarski, Phys. Rev. D **66**, 096003 (2002); A. Dumitru, Y. Hatta, J. Lenaghan, K. Orginos, and R. D. Pisarski, Phys. Rev. D **70**, 034511 (2004); A. Dumitru, R. D. Pisarski, and D. Zschiesche, Phys. Rev. D **72**, 065008 (2005).
[10] K. Fukushima, Phys. Lett. B **591**, 277 (2004).
[11] S. K. Ghosh, T. K. Mukherjee, M. G. Mustafa, and R. Ray, Phys. Rev. D **73**, 114007 (2006).
[12] E. Megías, E. R. Arriola, and L. L. Salcedo, Phys. Rev. D **74**, 065005 (2006).
[13] C. Ratti, M. A. Thaler, and W. Weise, Phys. Rev. D **73**, 014019 (2006).
[14] M. Ciminale, R. Gatto, N. D. Ippolito, G. Nardulli, and M. Ruggieri, arXiv:hep-ph/0711.3397; M. Ciminale, G. Nardulli, M. Ruggieri, and R. Gatto, Phys. Lett. B **657**, 64 (2007).
[15] C. Ratti, S. Rößner, M. A. Thaler, and W. Weise, Eur. Phys. J. C **49**, 213 (2007).
[16] S. Rößner, C. Ratti, and W. Weise, Phys. Rev. D **75**, 034007 (2007).
[17] H. Hansen, W. M. Alberico, A. Beraudo, A. Molinari, M. Nardi, and C. Ratti, Phys. Rev. D **75**, 065004 (2007).
[18] C. Sasaki, B. Friman, and K. Redlich, Phys. Rev. D **75**, 074013 (2007).
[19] W. J. Fu, Z. Zhang, and Y. X. Liu, Phys. Rev. D **77**, 014006 (2008).
[20] K. Kashiwa, H. Kouno, M. Matsuzaki, and M. Yahiro, arXiv:hep-ph/0710.2180 [Phys. Lett. B (to be published)].
[21] M. Asakawa and K. Yazaki, Nucl. Phys. **A504**, 668 (1989).
[22] M. Kitazawa, T. Koide, T. Kunihiro, and Y. Nemoto, Prog. Theor. Phys. **108**, 929 (2002).
[23] K. Kashiwa, H. Kouno, T. Sakaguchi, M. Matsuzaki, and M. Yahiro, Phys. Lett. B **647**, 446 (2007); K. Kashiwa, M. Matsuzaki, H. Kouno, and M. Yahiro, Phys. Lett. B **657**, 143 (2007).
[24] G. Boyd, J. Engels, F. Karsch, E. Laermann, C. Legeland, M. Lütgemeier, and B. Petersson, Nucl. Phys. **B469**, 419 (1996).
[25] O. Kaczmarek, F. Karsch, P. Petreczky, and F. Zantow, Phys. Lett. B **543**, 41 (2002).
[26] B. J. Schaefer, J. M. Pawlowski, and J. Wambach, Phys. Rev. D **76**, 074023 (2007).